Cell, Vol. 118, 715–729, September 17, 2004, Copyright ©2004 by Cell Press

Mis16 and Mis18 Are Required for CENP-A Loading and Histone Deacetylation at Centromeres

Takeshi Hayashi,[1,2] Yohta Fujita,[1,2] Osamu Iwasaki,[1] Yoh Adachi,[1] Kohta Takahashi,[1,3] and Mitsuhiro Yanagida[1,*]
[1]Department of Gene Mechanisms
Graduate School of Biostudies
Kyoto University
Sakyo-ku, Kyoto 606-8502
Japan

Summary

Centromeres contain specialized chromatin that includes the centromere-specific histone H3 variant, spCENP-A/Cnp1. Here we report identification of five fission yeast centromere proteins, Mis14–18. Mis14 is recruited to kinetochores independently of CENP-A, and, conversely, CENP-A does not require Mis14 to associate with centromeres. In contrast, Mis15, Mis16 (strong similarity with human RbAp48 and RbAp46), Mis17, and Mis18 are all part of the CENP-A recruitment pathway. Mis15 and Mis17 form an evolutionarily conserved complex that also includes Mis6. Mis16 and Mis18 form a complex and maintain the deacetylated state of histones specifically in the central core of centromeres. Mis16 and Mis18 are the most upstream factors in kinetochore assembly as they can associate with kinetochores in all kinetochore mutants except for *mis18* and *mis16*, respectively. RNAi knockdown in human cells shows that Mis16 function is conserved as RbAp48 and RbAp46 are both required for localization of human CENP-A.

Introduction

Recent progress in the molecular cell biology of kinetochores shows that despite divergence in the DNA content, size, and sequence of centromeres, the groups of proteins that associate with kinetochores are surprisingly conserved in evolution. This poses the intriguing question as to how conserved kinetochore proteins can assemble on a wide range of DNA sequences. A number of kinetochore proteins have been identified in model organisms. Some interact with kinetochore microtubules and provide the link between the spindle and chromosomes that is necessary to enable the separated sister chromatids to opposite spindle poles. Others are required to generate the unique chromatin structure that is found at centromeres and is essential for equal segregation.

CENP-A is the kinetochore-specific histone H3 that is thought to be a component of kinetochore-specific nucleosomes. CENP-A was initially identified as a human kinetochore-specific antigen and later found to be a histone H3 variant that is essential for equal segregation (Earnshaw and Migeon, 1985; Palmer et al., 1987; Henikoff et al., 2000; Takahashi et al., 2000; Measday et al., 2002). This H3 variant is present from lower eukaryotes to vertebrates and associates with kinetochores in all systems analyzed to date. For example the budding yeast cenpA-related protein Cse4 is a kinetochore-specific histone H3 variant (Stoler et al., 1995) that is essential for viability and chromosome segregation.

The centromeric DNA of fission yeast is repetitive and complex. A series of outer repeats (otr) flank inner repeats (imr) that surround a central nonrepetitive region (cnt). The fission yeast cenpA-like kinetochore-specific histone H3, spCENP-A (designated Cnp1), is present in the central domain (imr and cnt) of the centromeres but not in the outer repetitive heterochromatic regions (Takahashi et al., 2000; Chen et al., 2003). The specialized chromatin of the central domains changes its structure when temperature-sensitive mutants in *cnp1* and some other kinetochore proteins are cultured at the restrictive temperature (Saitoh et al., 1997; Goshima et al., 1999; Jin et al., 2002; Pidoux et al., 2003). As a result, chromosomes segregate unequally.

Mis12/Mtw1, a member of another evolutionarily conserved kinetochore protein family, is required for accurate chromosome segregation in both fission and budding yeasts (Goshima and Yanagida, 2000). Fission yeast genetics and RNAi in tissue culture cells suggest that the Mis12 and CENP-A recruitment pathways are independent and that loading of either protein alone is not sufficient for correct segregation (Goshima et al., 1999, 2003; Takahashi et al., 2000).

To improve our understanding of the pathways that recruit kinetochore proteins, we isolated new mutants that interfere with chromosome segregation. These mutants identify five new genes involved in kinetochore function. Two of them, Mis16 and Mis18, are required for the loading of CENP-A and form a complex. Human homologs of Mis16 are thought to influence chromatin assembly and remodeling. In addition, we show that acetylated histones accumulate in the central domains of the centromeres in *mis16* and *mis18* mutants but not in wild-type cells. Mis16 and Mis18 therefore appear to be required to ensure that the histones in the central domains of the centromeres are maintained in a deacetylated state.

Results

Seven New ts Mutants Revealed Unequal Segregation at 36°C

One thousand fifteen temperature-sensitive (ts) mutants were isolated by replica plating after nitrosoguanidine (150 μg/ml) mutagenesis. Individual strains were grown at 26°C and then shifted to 36°C for 2–5 hr. Cells were stained with DAPI, a fluorescent DNA probe, and observed under a fluorescence microscope. Seven mutants (53, 68, 262, 271, 362, 634, 818) displayed a chro-

*Correspondence: yanagida@kozo.lif.kyoto-u.ac.jp
[2]These authors contributed equally to this work.
[3]Present address: Division of Cell Biology, Institute of Life Science, Kurume University, 2432-3 Aikawa-machi, Kurume, Fukuoka, 839-0861, Japan.

A

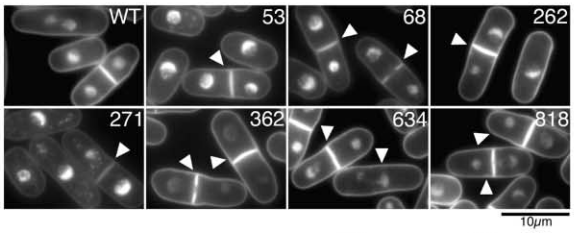

B

Gene	Allele	$ts^+ : ts^-$
mis14	271 , 634	2 : 2
mis15	68	2 : 2
mis16	53	2 : 2
mis17	362	2 : 2
mis18	262 , 818	2 : 2

C

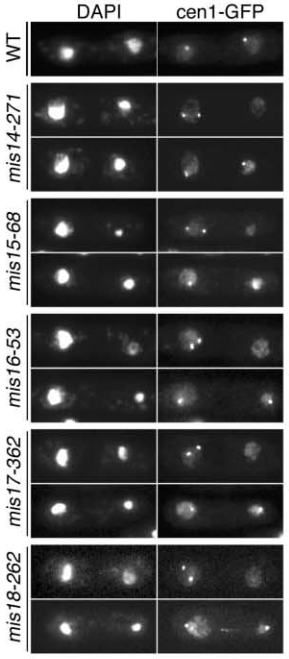

D

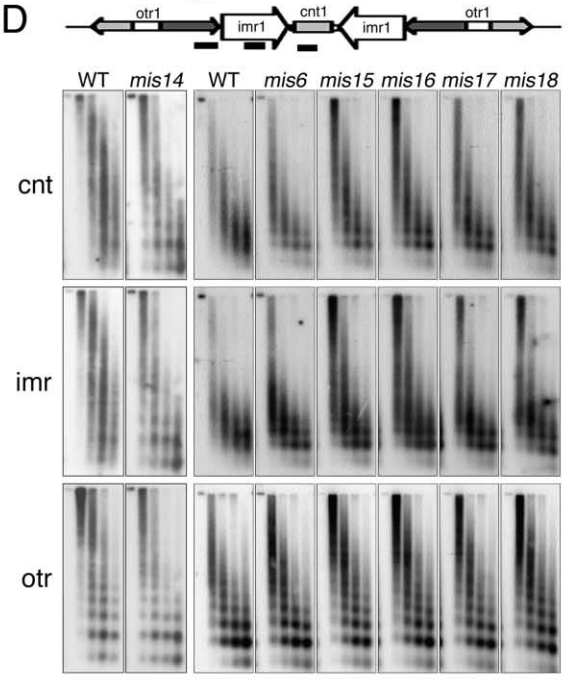

E

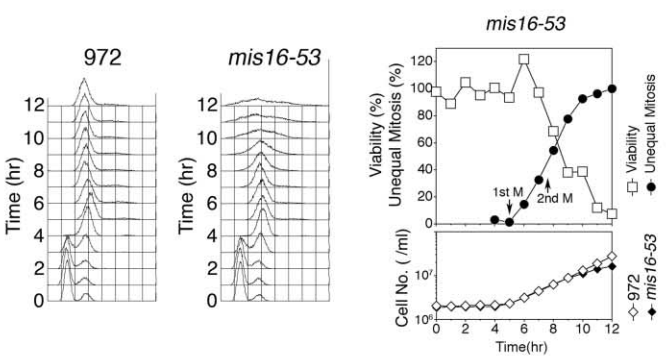

F

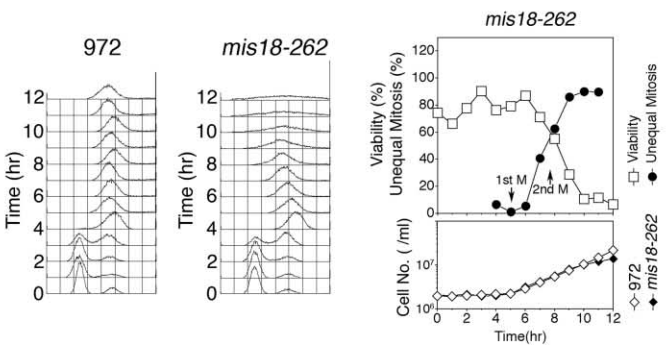

mosome missegregation phenotype that resulted in large and small daughter nuclei at 36°C (Figure 1A). Previous analysis of *mis6*, *mis12*, and *cnp1* has established that this phenotype is the hallmark of mutations in authentic kinetochore components (Saitoh et al., 1997; Goshima et al., 1999; Takahashi et al., 2000). These strains comprised five groups, designated, *mis14–271*, *-634*, *mis15–68, mis16–53, mis17–362*, and *mis18–262, -818* (Figure 1B). None of them was linked to any known loci.

The binding of GFP-labeled Lac repressor to a centromere-linked array of Lac operator repeats (Experimental Procedures) was used to confirm that the large and small daughter nuclear phenotypes were indeed due to unequal segregation of chromosomes. All of the seven strains cultured at 36°C showed a high frequency of chromosome missegregation (Figure 1C). Hence we concluded that the correct segregation of chromatids to opposite spindle poles requires the function of the Mis14–Mis18 proteins.

Specialized Centromere Chromatin Is Disrupted in *mis14–mis18*

The chromatin of the central centromere has an organization that is distinct from that of the outer repeats and the chromosome arms. This difference is revealed as a smeared digestion pattern upon micrococcal nuclease (MNase) of the central centromere as opposed to the nucleosome ladders seen on digestion of other chromatin. In order to analyze the structure of the chromatin in the centromeres of these novel mutants, nuclear chromatin was prepared from wild-type and *mis14–mis18* mutants cultured at 36°C for 8 hr and probed by micrococcal nuclease digestion (Figure 1D). The smeared pattern in the central centromere was greatly reduced in *mis14–mis18* mutants and replaced with the more ordered nucleosome ladders that are typical of the outer repeats. This suggested that Mis14–Mis18 were required for the formation or maintenance of specialized chromatin of centromeres. The small amount of smeared chromatin that persisted in the mutants was probably due to incomplete penetrance of the particular mutant alleles used.

Loss of Viability Coincides with Missegregation

We examined the phenotypes of the mutants in detail. We monitored the degree of unequal chromosome segregation, cell number, and viability of the mutant strains (*mis14–271, mis15–68, mis16–53, mis17–362*, and *mis18–262*) as the culture temperature was shifted to 36°C after long-term growth at 26°C. Binucleate cells containing large and small daughter nuclei reached 60%–80% after 6 hr in all mutants, as the viability declined to 20% (data not shown). The increase in cell number reached a plateau after increasing around 8-fold. This high frequency of unequal chromosome segregation generated aneuploid cells that could undergo a few rounds of division but lost viability.

We next asked when nitrogen-starved G1-arrested mutant cells would lose viability upon introduction into a nitrogen-rich complete medium under restrictive conditions (36°C) that would induce them to re-enter the cell cycle and commence log phase growth. FACS analysis confirmed that re-entry into the cell cycle and S phase was synchronous (Figures 1E and 1F, left panels for *mis16–53* and *mis18–262*, respectively). In the *mis16* mutant, the first mitosis (5 hr) was completely normal, and the unequal segregation of chromosomes occurred in the second mitosis (7–8 hr, right panel). Cell viability decreased as the second mitosis generated unequal chromosome segregation. Essentially the same results were obtained for *mis18–262* (Figure 1F), *mis14–271, mis15–68*, and *mis17–362* (data not shown). Therefore, in order for missegregation to occur, these mutant cells had to be continuously maintained at the nonpermissive temperature from the previous mitosis. In other words, kinetochore proteins had to be maintained in an inactive state from one mitosis until the next. Restoration of protein function at any point between two mitoses enabled cells to segregate their chromosomes correctly. These results suggest that kinetochore structure may be maintained throughout replication and that a single kinetochore can give rise to two functional daughter kinetochores without needing to recruit functional components that are not already part of the kinetochore. However it is possible that the first cycle after release from nitrogen starvation is slower than the second, and these mutants might only affect kinetochore function during rapid cell cycles.

Sequence Comparisons of the *mis14*$^+$–*mis18*$^+$ Genes and Their Gene Products

Gene cloning was done by transformation of mutant strains, and the mutant alleles were sequenced and the changes in amino acid sequence are depicted in Figures 2A–2D. Mis14 (Spac688.02c) shows weak similarity (23% identical) to the budding yeast *S. cerevisiae* Nsl1, a kinetochore protein (Figure 2A) that is also predicted

Figure 1. Unequal Segregation and Disruption of Specialized Centromere Chromatin in Seven ts Mutants

(A) DAPI-stained cells cultured at 36°C for 5 hr. Unequal sized daughter nuclei (arrowheads) were frequently observed in mutants (indicated by the strain number) but not in wild-type (WT).

(B) Linkage analysis established that the seven strains mapped to five loci.

(C) Mutant cells showing 1:1 segregation of CEN1-GFP revealed the missegregation of other chromosomes as they showed the large and small daughter nuclei by DAPI.

(D) Centromere-specific chromatin structure is disrupted in *mis14–mis18* mutant cells. Chromatin prepared from mutant cultures at 36°C for 8 hr was digested with MNase for 0, 1, 2, 4, and 8 min, followed by gel electrophoresis and Southern hybridization with the three centromere DNA probes, cnt, imr, and otr. The centromeric DNAs are depicted with the probes (the short bars) used.

(E and F) Unequal segregation occurs after the traverse of a pre-G1 stage. The *mis16–53* and *mis18–262* strains arrested by nitrogen starvation at 26°C were shifted to complete medium at 36°C. Left: Aliquots of the cultures were used for FACS analysis. The DNA content in wild-type *972* is also shown. S phase occurred around 4 hr. Right: The loss of viability (%), the unequal mitosis (%), and the increase in cell number are shown.

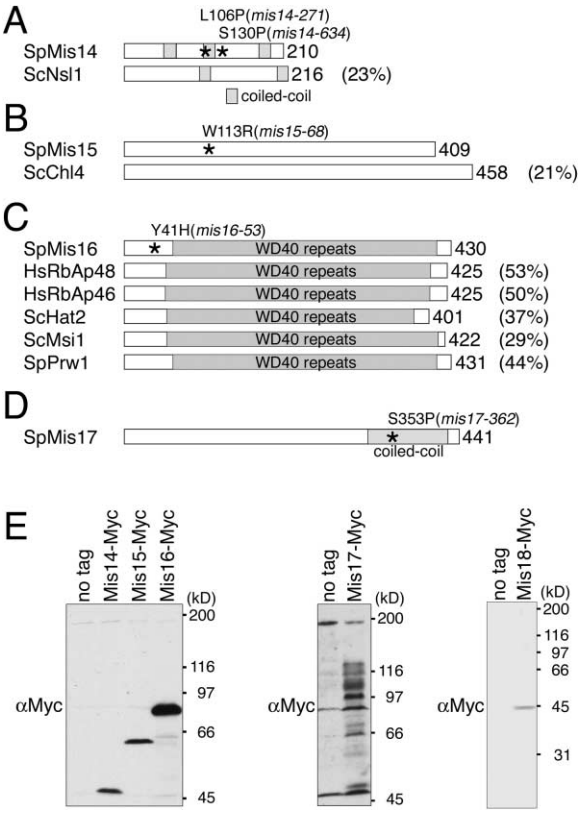

Figure 2. A Schematic Representation of Mis14–Mis17 Proteins

(A) Mis14 and budding yeast Nsl1.

(B) Mis15 and budding yeast Chl4.

(C) Mis16 is highly similar to human RbAp48 (53% identity) and RbAp46 (50%).

(D) Mis17 is a sequence orphan.

(E) Immunoblotting of *S. pombe* extracts expressing the Myc-tagged Mis14–Mis18 proteins. The tagged genes were chromosomally integrated and verified by Southern hybridization. The protein bands were observed at the expected positions. Mis17-myc produced multiple bands.

to contain coiled-coil motifs. Nsl1 genetically and physically interacts with Mtw1 (Euskirchen, 2002; Pinsky et al. 2003; Scharfenberger et al., 2003; Nekrasov et al., 2003; Westermann et al., 2003; De Wulf et al., 2003), a budding yeast homolog of fission yeast Mis12 (Goshima and Yanagida, 2000).

Mis15 (pi022; Figure 2B) exhibits weak similarity (21% identity) to the budding yeast Chl4/Mcm17/Ctf17, a kinetochore protein (Pot et al., 2003). Chl4/Mis15 has no established protein motif. Mis15 mutant protein contains the substitution W113R. This tryptophan residue is conserved in the *S. cerevisiae* and *Candida albicans* Chl4 proteins.

Sequence analysis of the Mis16$^+$ gene (Spcc1672.10) predicts seven WD repeats (Figure 2C) and similarity to human RbAp46 and RbAp48 (50%–53% identity). The sequence of *S. pombe* Prw1, a component of the Clr6-containing histone deacetylase complex (Nakayama et al., 2003), exhibits 44% identity with the predicted sequence of Mis16. In addition to Prw1, the histone deacetylase complex contains Alp13, Clr6, and Pst2; Clr6 is the catalytic subunit. Budding yeast Hat2 also exhibits similarity (33%–37% identity) to Prw1 and Mis16. Disruption of the *mis16*$^+$ gene by one-step replacement showed that the *mis16*$^+$ gene was essential for cell viability. The Ura$^+$ *mis16* null spores germinated and frequently (more than 50%) displayed severe unequal segregation of the chromosomes before they ceased cell division (Supplemental Figure S1 at http://www.cell.com/cgi/content/full/118/6/715/DC1). As the *prw1*$^+$ gene is not essential (Nakayama et al., 2003) and a plasmid carrying the *prw1*$^+$ gene failed to rescue the ts phenotype of *mis16* (data not shown), Prw1 and Mis16 execute distinct functions.

Mis17 (Spbc21.01) is serine rich and a sequence orphan (Figure 2D). Mis18 (Spcc970.12) failed to give any indication of any characterized functional domains. Gene disruption indicated that *mis18*$^+$ was essential for cell viability (data not shown). Gene-disrupted cells frequently ($\sim$30%) produced the unequal sized nuclei (Supplemental Figure S2 on *Cell* website). Mis18 has homologs in vertebrates (e.g., human C21ORF45 and OIP5 designated hMis18α, β, respectively).

In order to identify and study the protein products of *mis14*$^+$–*mis18*$^+$ genes, the products' chromosomal genes were tagged with 8myc epitopes at the C terminus by a standard replacement method. The tagged genes were functionally equivalent to the wild-type genes as they did not appear to induce any defects in mitosis. As seen in Figure 2E, the Myc-tagged Mis14, Mis15, and Mis16 were detected in extracts of the integrant strains by immunoblotting. The level of Mis16-myc was the highest of all these molecules. Mis17-myc produced many bands ranging from 50 to 120 kDa. It is probable that Mis17 is modified. Myc-tagged Mis18 is also shown.

Kinetochore and Nuclear Localization of Chromosomally Integrated Mis14–Mis17 GFP Fusions

GFP (green fluorescent protein) was inserted in-frame at the C termini of Mis14–Mis17. Each of the resulting tagged genes with the native promoter was integrated into the chromosome to replace the wild-type gene. Southern hybridization confirmed the correct integration. As shown in Figure 3A, the GFP signals for Mis14 were clustered into a single dot in interphase and became dispersed into multiple spots in mitotic cells. This distribution is indistinguishable from that of established kinetochore proteins (Saitoh et al., 1997; Goshima et al., 1999). The images obtained for Mis15-GFP and Mis17-GFP were identical to those of Mis14-GFP, suggesting that Mis15-GFP and Mis17-GFP were located at the kinetochores (Figures 3B and 3D). In sharp contrast, GFP-tagged Mis16 was enriched in the whole nuclear chromatin region throughout the cell cycle (Figure 3C). At 36°C, additional kinetochore/SPB (spindle pole body) dots were particularly clear in the interphase. In mitosis, a diffuse GFP labeling pervaded the whole nucleus.

Mis14–Mis17 Proteins Bound to the Central Region of Centromeres

Chromatin immunoprecipitation (CHIP) was done using centromere DNA probes to determine whether Mis14–Mis17 proteins bound to centromeres (Saitoh et al., 1997; Goshima et al., 1999). Chromosomally integrated Myc-tagged Mis14–Mis17 were immunoprecipitated by anti-Myc antibodies, followed by the PCR amplification

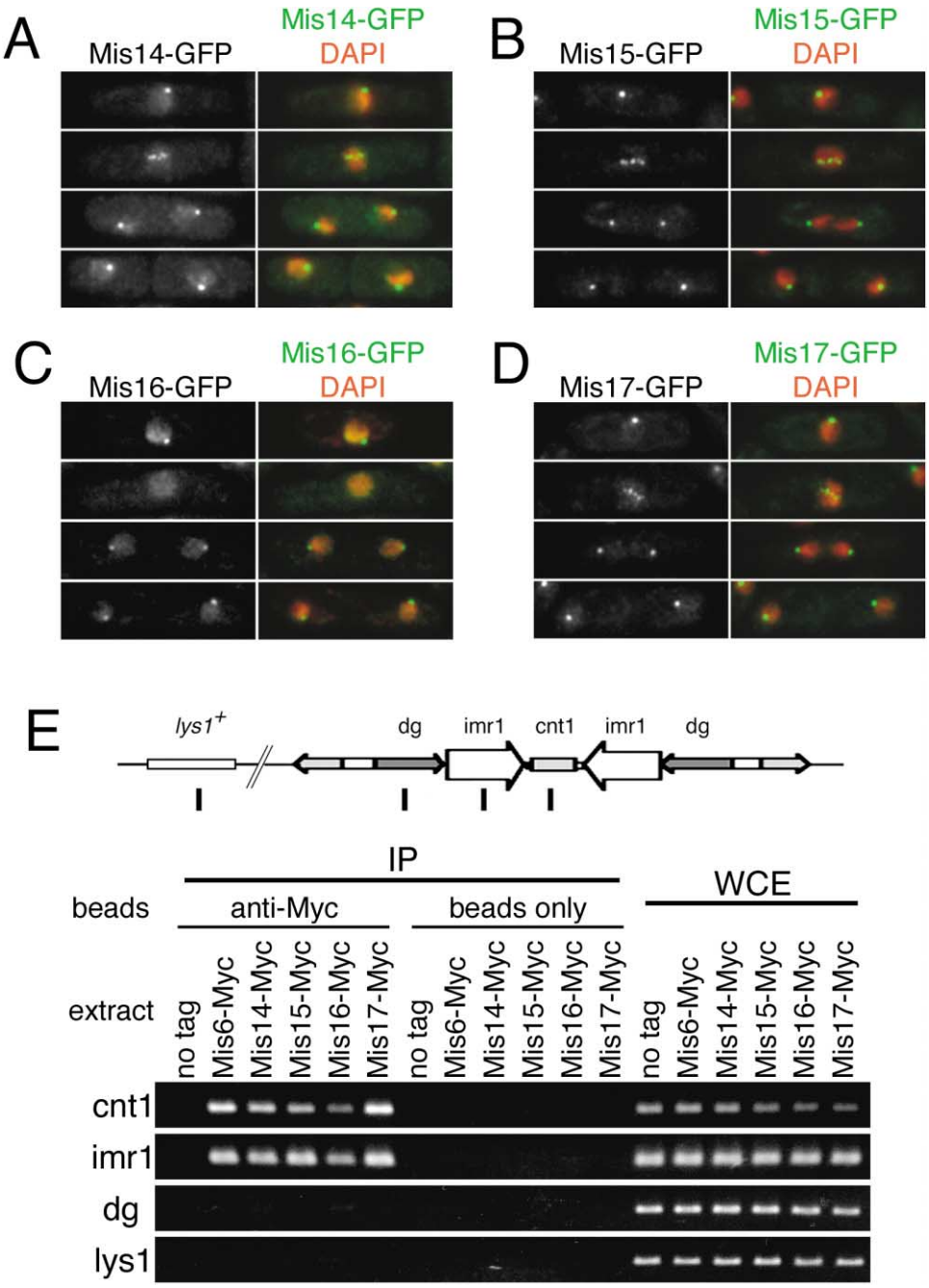

Figure 3. Kinetochore Localization and Central Centromere DNA Association of Mis14, Mis15, Mis16, and Mis17

(A–D) Localization of GFP-tagged Mis14–Mis17 expressed by the chromosomally integrated genes. (A) Mis14-GFP, (B) Mis15-GFP, (C) Mis16-GFP, (D) Mis17-GFP. DAPI was used for counter stain.

(E) Chromatin immunoprecipitation (CHIP) was done for chromatin preparations of cells expressing Mis14–Mis17 tagged with the myc epitope. The centromere probes used were cnt1, imr1, and dg while pericentric probe lys1 was also used (their genomic localizations indicated below by vertical lines). Tagged Mis6 was used as a positive control.

of the precipitates with appropriate DNA probes alongside a strain in which chromosomally integrated Mis6 was precipitated as a positive control. As shown in Figure 3E, immunoprecipitates of Myc-tagged Mis14–Mis17 contained the central centromeric DNAs such as cnt1 and imr1, but not the outer centromeric sequence dg and the pericentric marker lys1. These results established that the kinetochore proteins Mis14–Mis17 were predominantly localized to the central centromere DNA regions.

High-Copy Suppression and Synthetic Lethal Interactions amongst *mis* Mutants

We next assessed the relationship between the different kinetochore components by asking whether an increase in gene dosage of one component could suppress the

defect in mutations in other genes. To this end, plasmids carrying the *cnp1*$^+$, *mis6*$^+$, *mis12*$^+$, *mis14*$^+$–*mis18*$^+$ genes were individually introduced into *cnp1*, *mis6*, *mis12*, or *mis14–mis18* mutant strains and the transformants plated at the restrictive (33°C –36°C) and permissive (22°C–26°C) temperatures (Figure 4A). Elevating *cnp1*$^+$ gene dosage with the high copy number plasmid pCNP1 weakly suppressed the ts phenotype of *mis6, mis15, mis16, mis17*, and *mis18* mutants, while increasing *mis6*$^+$ gene dosage did not suppress any mutants tested. Plasmid pMIS12 suppressed two *mis14* alleles. Conversely, pMIS14 suppressed the ts phenotype of *mis12–537*: high-copy suppression of *mis12* and *mis14* was thus mutual. These results are represented schematically in Figure 4A (the arrows indicate suppression).

Synthetic genetic interactions were found between *mis12* and *mis14*: both *mis12–537 mis14–271* and *mis12–537 mis14–634* double mutants were lethal at 30°C (data not shown). Other synthetic interactions were found for *mis6, mis15*, and *mis16*: three double mutants *mis6–302 mis15–68*, *mis15–68 mis16–53*, and *mis6–302 mis16–53* were lethal at 30°C.

Physical Interactions amongst Kinetochore Proteins

The above results indicated that the functions of Mis12 and Mis14 and Cnp1, Mis6, Mis15, Mis16, and Mis17 were closely related. We therefore used a coimmunoprecipitation assay to ask whether Mis6, Mis12, Mis14–Mis17 physically interacted with each other. For this purpose, strains in which HA-tagged Mis6 and Myc-tagged Mis14–Mis17 genes had been integrated at the native loci were employed. Anti-Myc immunoprecipitates were immunoblotted with polyclonal anti-Mis12, anti-Myc, and anti-HA antibodies (Figure 4B). Mis12 coimmunoprecipitated with Mis14-Myc, while Mis6-HA coimmunoprecipitated with Mis15-Myc and Mis17-Myc. Furthermore, Mis15-HA coprecipitated with Mis17-Myc (Figure 4C). These results indicated that Mis14 and Mis12 formed a complex, while Mis6, Mis15, and Mis17 formed a second distinct complex in cell extracts. We did not detect any stable association of Mis16 with any of these proteins. The results of physical interactions are summarized in Figure 4D.

Localization Dependencies of Kinetochore Proteins

In order to analyze how these kinetochore proteins were recruited to kinetochores in different genetic backgrounds, we constructed eight strains in which the *cnp1*$^+$, *mis6*$^+$, *mis12*$^+$, *mis14*$^+$–*mis18*$^+$ genes were tagged with GFP under the control of their native promoter and crossed them with kinetochore mutants. GFP signals were observed in resulting strains at the restrictive (36°C) and the permissive (20°C) temperatures (Figures 5A–5H).

The kinetochore dot localization of spCENP-A was maintained in a *mis14* mutant but greatly diminished (10%–20% dot frequencies) in *mis15, mis16, mis17*, and *mis18* mutants at 36°C (Figure 5A). The frequency with which dots could be seen was scored and plotted to give the graphs to the right of the micrographs for each set of experiments. Note that GFP observation was carried out at a single focal plane so that the signals of GFP could not be seen in a fraction of cells in which the centromeres were out of focus. The signal for spCENP-A was diffused throughout the nucleus in *mis15, mis16, mis17*, and *mis18* mutants, indicating that the kinetochore localization of CENP-A was impaired in these strains. For Mis6-GFP, the proportion of the culture that exhibited dot staining was further reduced to less than 5% and the signal was diffused throughout the nucleus in *mis15, mis16, mis17*, and *mis18* mutants at 36°C (Figure 5B). However, Mis6-GFP remained as a dot in a *mis14* mutant. These results showed that Mis15–Mis18 were required for the association of Mis6 and spCENP-A with kinetochores.

The frequency with which Mis12-GFP dots could be seen was reduced (25%) in *mis14* mutant cells but unaffected in all other mutants (Figure 5C). The localization of Mis14-GFP signals was then tested in wild-type and kinetochore mutants (Figure 5D). The kinetochore localization of Mis14-GFP was diminished (25% cells) in a *mis12* mutant but normal in other mutants. This demonstrated that Mis14 and Mis12 were mutually dependent upon one another for kinetochore localization, which is consistent with their association in the same complex. Mis12 and Mis14 were thus recruited to kinetochores, independently of defects in the functions of CENP-A, Mis6, Mis15, Mis16, Mis17, or Mis18.

Kinetochore localization of Mis15-GFP was abolished ($<$5% cells) in a *mis16* mutant and diminished in *mis17, mis18, mis6*, and *cnp1* mutants (Figure 5E). In *mis12* and *mis14* mutants, the frequency of cells with Mis15-GFP kinetochore staining was similar to that of wild-type cells. For Mis17-GFP, similar localization data were obtained in different genetic backgrounds (Figure 5G).

These results established that Mis16 and Mis18 were needed for the recruitment of spCENP-A, Mis6, Mis15, and Mis17 to kinetochores. As the levels of Cnp1, Mis6, and Mis15 proteins were similar in *mis16* and wild-type cells (Figure 6B and data not shown), the failure in association with kinetochores was not due to the loss of these proteins in *mis16* mutant. The kinetochore localization of the Mis6, Mis15, and Mis17 complex may be facilitated by Mis16 and Mis18. Kinetochore recruitment of Mis15, Mis16, Mis17, and Mis18 was only slightly affected by mutation of *cnp1*. Because Mis12 and Mis14 could be recruited to kinetochores, we conclude that the kinetochore structure was partially retained in *mis16* and *mis18* mutants at 36°C.

The kinetochore dot-like signals of Mis16-GFP were prominent in cells at 36°C and less obvious at low temperature (20°C): Mis16-GFP was seen throughout nuclear chromatin at 20°C. With the exception of *mis18*, none of the kinetochore mutations affected the punctate nature of Mis16-GFP fluorescence (Figure 5F). Conversely, the dot localization of Mis18-GFP was only abolished in *mis16* mutants (Figure 5H). These results strongly suggested that Mis16 and Mis18 act at the most upstream level of the kinetochore recruitment pathway for Cnp1, Mis6, Mis15, and Mis17. Mis16 and Mis18, respectively, failed to be properly loaded in *mis18* and *mis16* mutant cells. A summary of dependency relationships between kinetochore proteins with respect to association with the kinetochore (indicated by the arrows) is shown in Figure 5I.

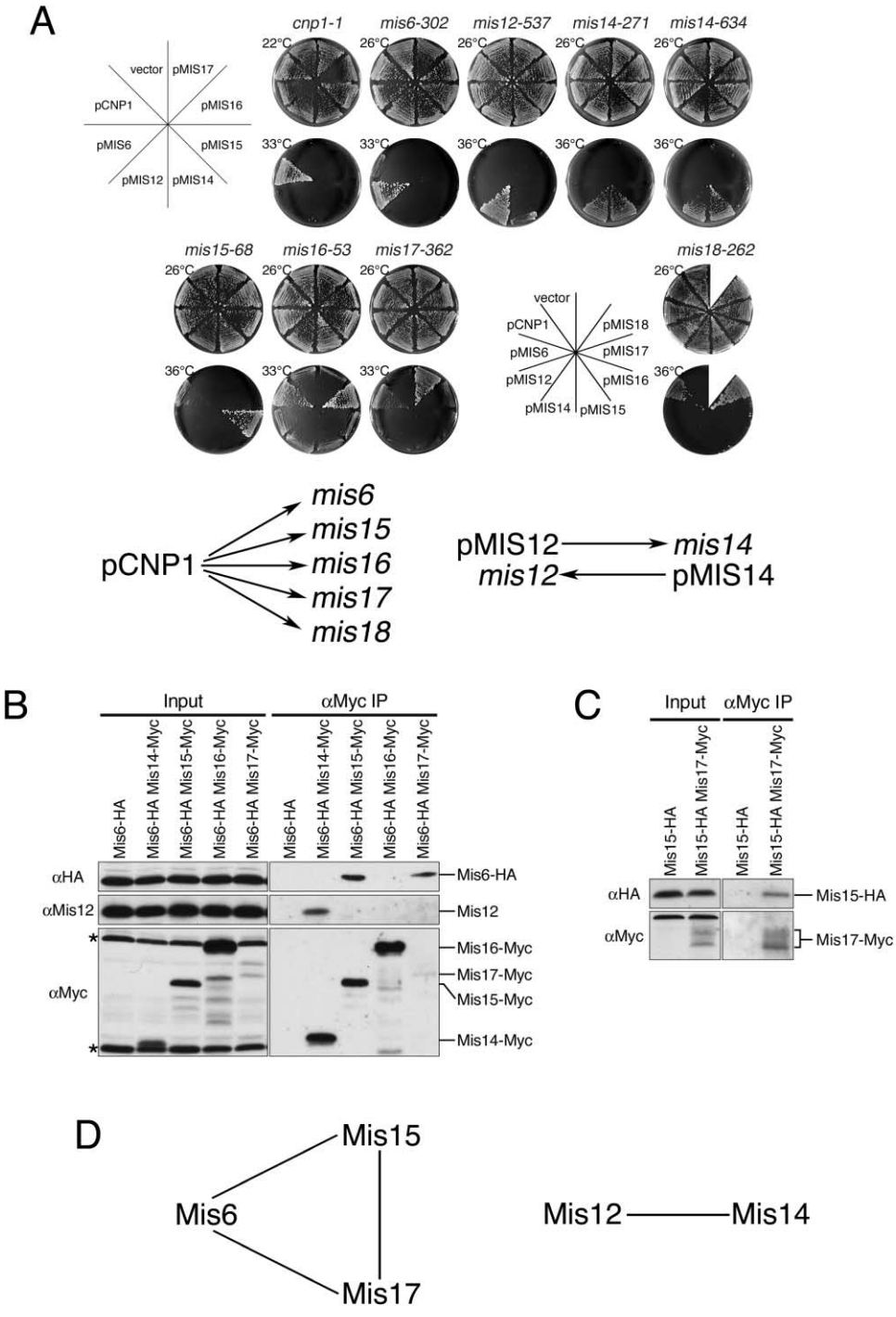

Figure 4. Genetic and Physical Interactions of Mis14–Mis17

(A) High-copy suppression of *mis* mutants by plasmids carrying the centromere protein genes. Eight mutants (indicated above the plates) contained one of plasmids carrying the genes indicated and plated at 22°C, 26°C, 33°C, or 36°C. The genetic interactions are schematized by arrows.

(B) Extracts of *S. pombe* cells expressing Mis6-HA and the indicated Myc-tagged proteins were immunoprecipitated by anti-Myc antibody. Precipitated materials were then immunoblotted, using antibodies against HA, Myc, and Mis12.

(C) Two strains expressing Mis15-HA or both Mis15-HA and Mis17-Myc were immunoprecipitated by anti-Myc antibodies. Mis15-HA was coimmunoprecipitated with Mis17-Myc.

(D) A summary of physical interactions observed is depicted.

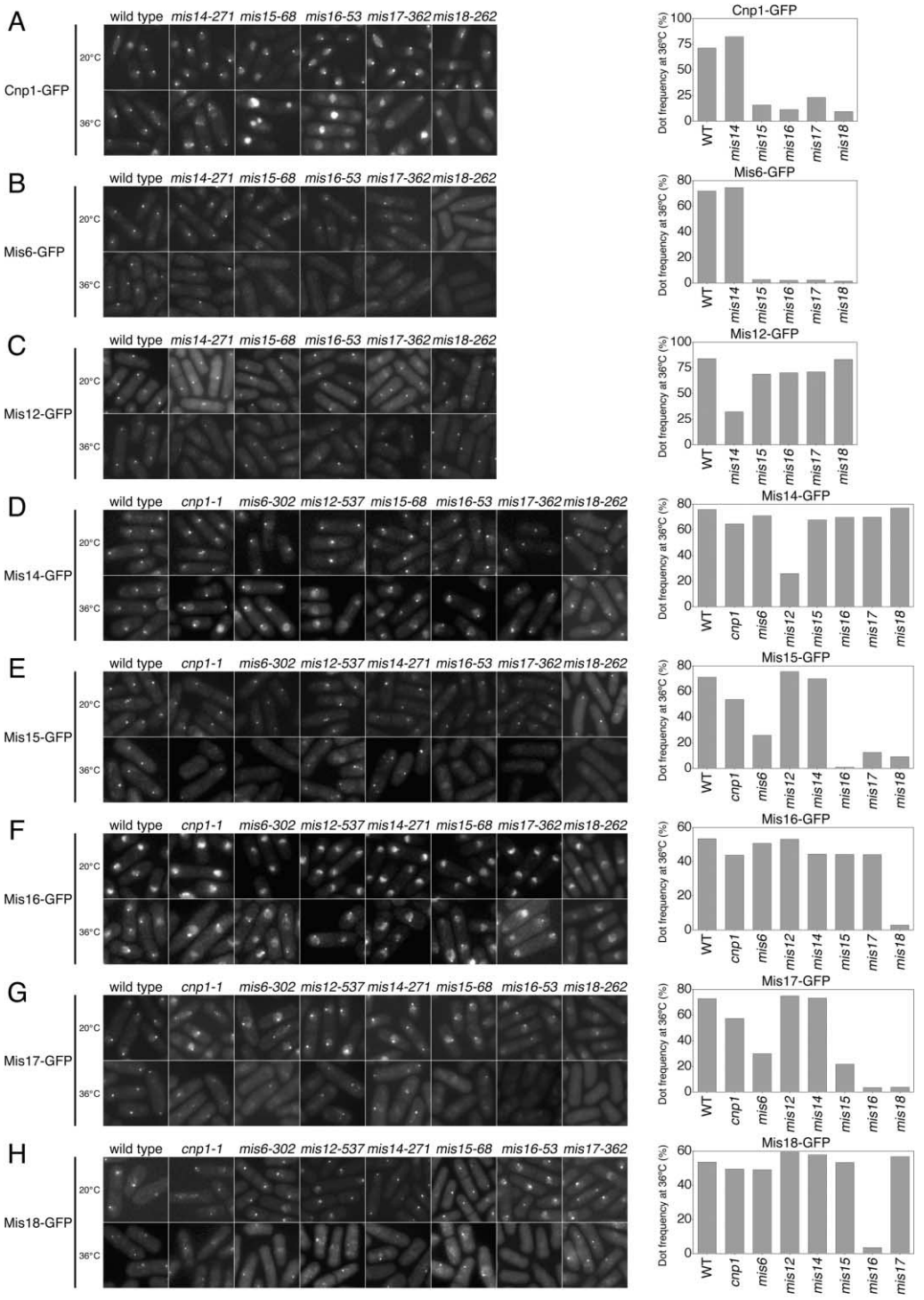
A
wild type mis14-271 mis15-68 mis16-53 mis17-362 mis18-262
Cnp1-GFP
20°C
36°C
Cnp1-GFP
Dot frequency at 36°C (%)
WT mis14 mis15 mis16 mis17 mis18
B
wild type mis14-271 mis15-68 mis16-53 mis17-362 mis18-262
Mis6-GFP
Mis6-GFP
C
wild type mis14-271 mis15-68 mis16-53 mis17-362 mis18-262
Mis12-GFP
Mis12-GFP
D
wild type cnp1-1 mis6-302 mis12-537 mis15-68 mis16-53 mis17-362 mis18-262
Mis14-GFP
WT cnp1 mis6 mis12 mis15 mis16 mis17 mis18
E
wild type cnp1-1 mis6-302 mis12-537 mis14-271 mis16-53 mis17-362 mis18-262
Mis15-GFP
WT cnp1 mis6 mis12 mis14 mis16 mis17 mis18
F
wild type cnp1-1 mis6-302 mis12-537 mis14-271 mis15-68 mis17-362 mis18-262
Mis16-GFP
WT cnp1 mis6 mis12 mis14 mis15 mis17 mis18
G
wild type cnp1-1 mis6-302 mis12-537 mis14-271 mis15-68 mis16-53 mis18-262
Mis17-GFP
WT cnp1 mis6 mis12 mis14 mis15 mis16 mis18
H
wild type cnp1-1 mis6-302 mis12-537 mis14-271 mis15-68 mis16-53 mis17-362
Mis18-GFP
WT cnp1 mis6 mis12 mis14 mis15 mis16 mis17
I
Mis16 ⇄ Mis18
Mis15 ⇄ Mis17
Mis6
Cnp1
Mis12 ⇄ Mis14

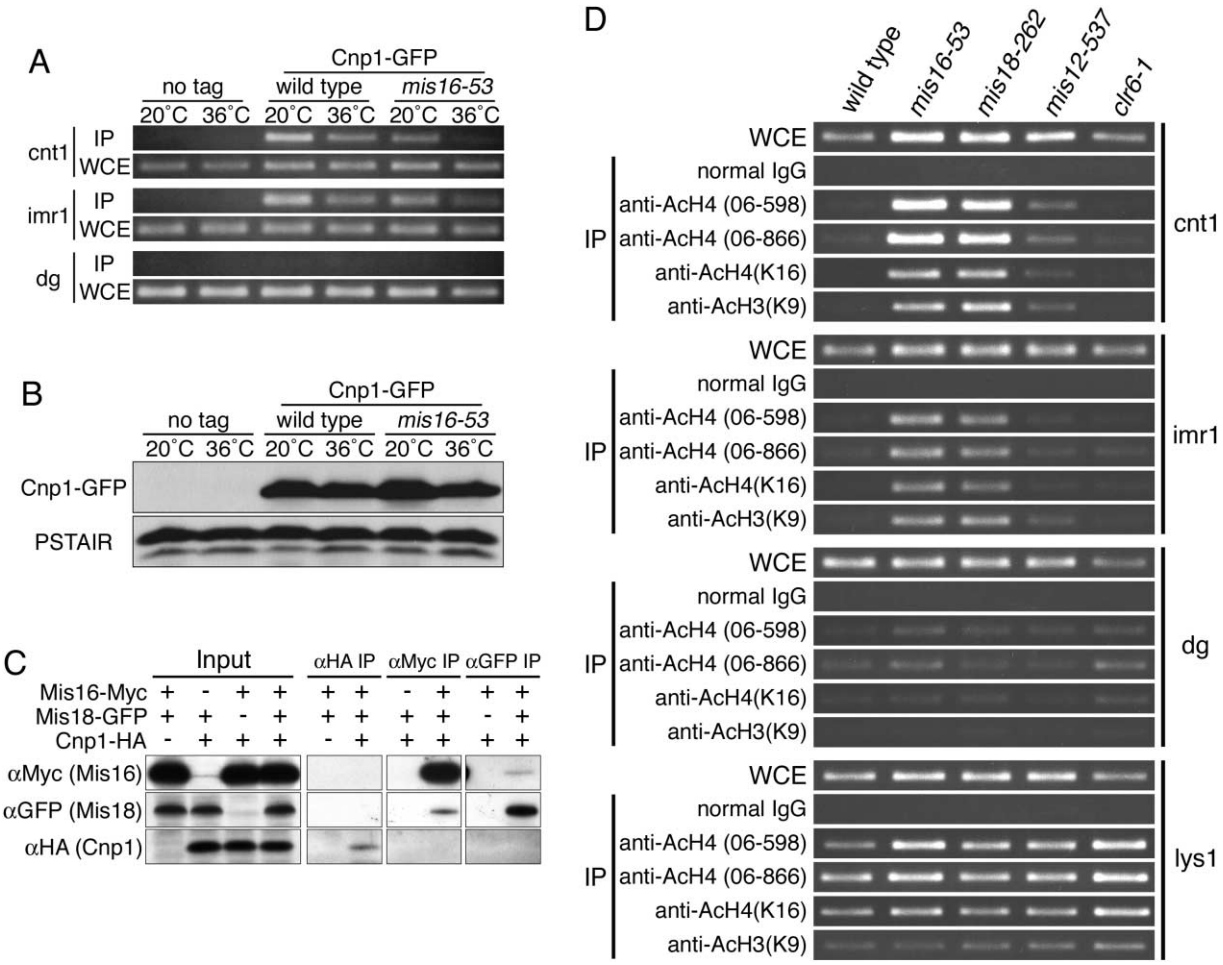

Figure 6. Histone Deacetylation Patterns in the Centromeric Regions Are Greatly Altered in *mis16* and *mis18* Mutants

(A and B) Cnp1 fails to associate with centromeres at 36°C in a *mis16* mutant in which a Cnp1-GFP gene fusion is integrated into the chromosome. A CHIP experiment was performed using the central centromere probes of cnt1, imr1, and the outer centromeric repeat dg (A). The amount of cnt1 and imr1 DNAs coprecipitated with the Cnp1-GFP fusion was reduced in *mis16* mutant cells at 36°C. The level of Cnp1-GFP protein was virtually identical in the wild-type and mutant strains at 36°C (B).

(C) Mis16 physically interacts with Mis18 but not with Cnp1. Mis16-Myc, Mis18-GFP, and Cnp1-HA that were chromosomally integrated were expressed under the control of the native promoter and immunoprecipitated (IP) using antibodies against Myc, GFP, and HA. The tagged Mis16 and Mis18 were detected in the precipitates of Mis18 and Mis16, respectively. The tagged Cnp1 protein was not detected in the precipitates of Mis16 and Mis18.

(D) The level of histones H3 and H4 acetylation in the central centromere. CHIP experiment was done for the centromere regions using antibodies against acetylated H3 and H4. Anti-AcH4 (06–598) and (06–866) were against acetylated K5, K8, K12, K16 in H4, while two other antibodies were against acetylated H4 K16 and H3 K9. The centromere probes used were central cnt1, imr1, and outer dg while pericentric probe lys1 was also used. Indicated strains were cultured at the restrictive temperature (36°C) for 8 hr.

Cnp1 Fails to Associate with Centromeres in *mis16–53*

In order to confirm that Cnp1 was absent from the centromeres of *mis16* mutant cells, we performed a CHIP (chromatin immunoprecipitation) experiment and immunoprecipitated GFP-tagged Cnp1 with anti-GFP antibodies from *mis16–53* cells. In mutant extracts cultured at 20°C, the central centromere probes cnt1 and imr1 coprecipitated as they did in wild-type cells, but coprecipitation was barely detectable at 36°C (Figure 6A). An immunoblot with anti-GFP antibodies demonstrated that the apparent reduction in association at 36°C was indeed due to a decrease in association rather than to destruction of the Cnp1 fusion protein at 36°C (Figure 6B).

Figure 5. Recruiting Pathways for Kinetochore Proteins

Localization of GFP-tagged and chromosomally integrated Cnp1 (spCENP-A), Mis6, Mis12, and Mis14–Mis18 with the native promoter was determined in various mutant backgrounds (*cnp1, mis6, mis12, mis14–mis18*). Each strain was grown at the permissive temperature and then shifted to the restrictive temperature for 8 hr. Quantitation of the frequency of cells with punctate dot staining in wild-type (WT) and different mutants are shown on the right. Kinetochore localization of Cnp1 (A), Mis6 (B), Mis12 (C), Mis14 (D), Mis15 (E), Mis16 (F), Mis17 (G), and Mis18 (H). (I) A schematic representation of the kinetochore localization dependency (indicated by arrows).

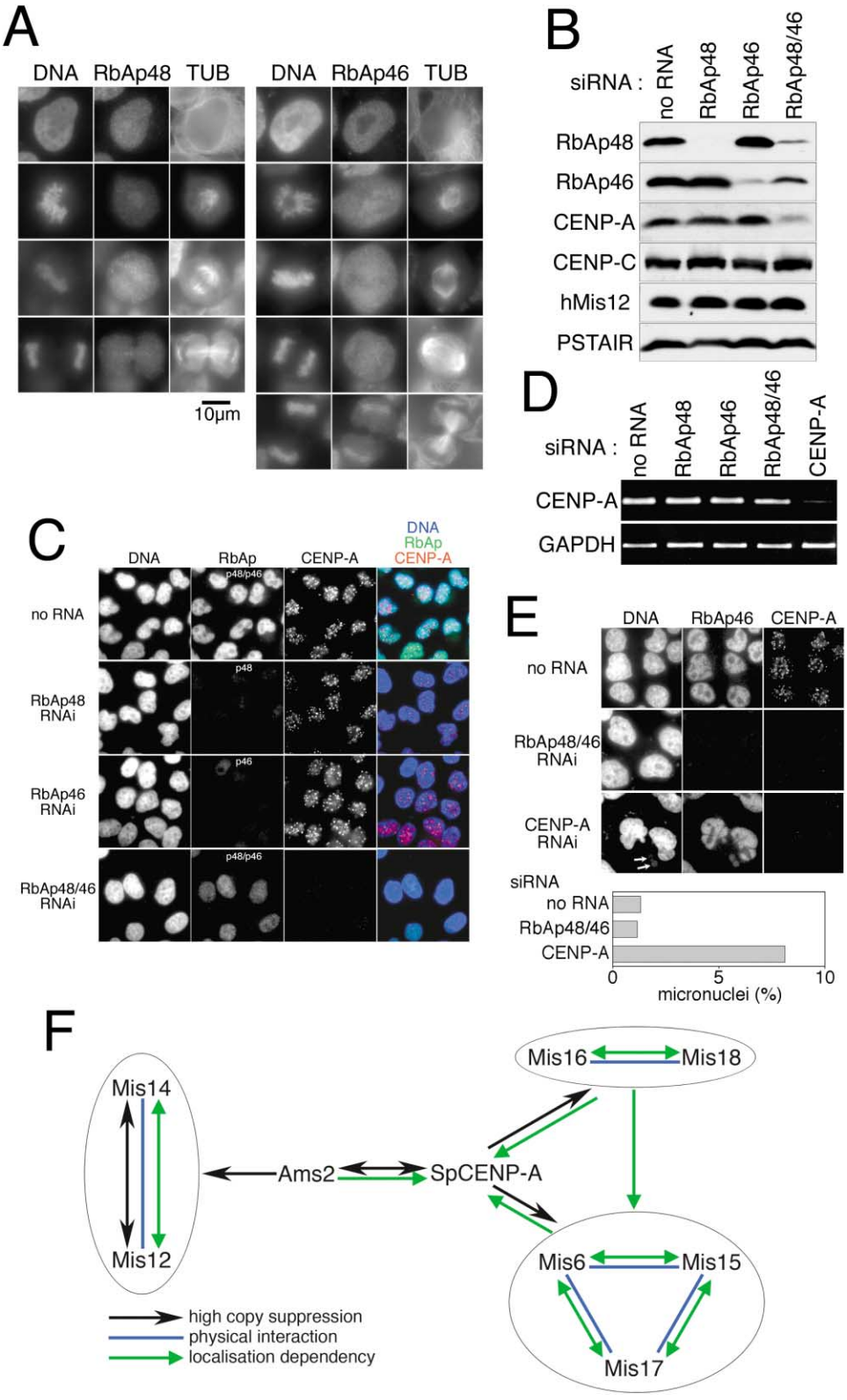

Figure 7. Human RbAp46 and RbAp48 Are Required for Kinetochore Localization of CENP-A

(A) Immunolocalization of RbAp48 and RbAp46. Hoechst 33342 and anti-tubulin antibody were used, respectively, for staining DNA and tubulin.

(B) Single and double RNAi were done in HeLa cells for 72 hr using specific siRNAs. The levels of RbAp46 and RbAp48 were assayed by immunoblot using specific antibodies.

(C) HeLa cells were immunostained with antibodies against RbAp48 or RbAp46 or both and CENP-A. The signals of CENP-A were greatly reduced in HeLa cells following simultaneous RNAi treatment against both RbAp46 and RbAp48.

Mis16 Physically Interacts with Mis18 but Not with CENP-A

As Mis16 localization was dependent upon that of Mis18 and vice versa, we asked whether the Mis16 and Mis18 proteins physically associated with one another. Strains were constructed in which the genes of Myc-tagged Mis16, GFP-tagged Mis18, and/or HA-tagged Cnp1 were chromosomally integrated and expressed under the control of a native promoter. Extracts by 0.2 M NaCl were prepared and immunoprecipitated either by anti-Myc, anti-GFP, or anti-HA antibody. As shown in Figure 6C, immunoprecipitation using antibodies against Myc or GFP established that GFP-tagged Mis18 formed a complex with Myc-tagged Mis16. However, within the sensitivity limits of the assay, we did not detect any coprecipitation of Cnp1 with Mis16 or Mis18.

A Marked Increase in the Level of Histone H3 and H4 Acetylation in the Central Centromeres of *mis16* and *mis18* Mutants

We used chromatin immunoprecipitation to examine the acetylation of the centromeric histones in *mis16* and *mis18* mutant cells. We probed histone binding to the central cnt1, imr1, and outer dg regions using antibodies that recognized acetylated K5, K8, K12, and K16 of histone H4 and acetylated K16 of histone H4 and K9 of histone H3. Wild-type, *mis16*, and *mis18* cells were processed after 8 hr at 36°C alongside the control strains *mis12* and *clr6*. The central centromere DNA probes showed a marked increase in the ability of this region to coprecipitate with acetylated H4 and H3 in *mis16* and *mis18* mutants over the behavior seen in wild-type cells. Such a striking difference in histone acetylation between wild-type and *mis16* (or *mis18*) mutants did not occur in the outer centromere region dg or the lys1 locus as no difference was seen in the levels of histone acetylation between wild-type and *mis16* or *mis18* cells. In the *mis12* mutant, acetylated histones were slightly more abundant in the central centromere than in wild-type. In the control *clr6* mutant, no change occurred in the central centromere, but the levels of acetylation were slightly enhanced in the outer dg and lys1 regions.

The increase of hyperacetylated H3 in the central centromeres of *mis16* and *mis18* mutants could indicate that Cnp1 (CENP-A) has been replaced with regular acetylated histone H3. When considered alongside the striking increase of acetylated histone H4 in the central centromeres in the same mutants, it is clear that there is a marked change in chromatin structure in the central but not outer centromere regions when the function of Mis16 or Mis18 is compromised. These data strongly support the view that Mis16 and Mis18 play an important role in maintaining the level of deacetylated histones specifically within the central core region of centromeres.

Human Mis16-like Proteins Are Required for CENP-A Kinetochore Localization

Two human proteins RbAp46 and RbAp48 (retinoblastoma-associated protein; Qian et al., 1993; Qian and Lee, 1995) are highly related (50%–53% identity) to *S. pombe* Mis16. Specific antibodies against RbAp46 and RbAp48 (purchased from Calbiochem) were employed for immunolocalization and immunoblotting in HeLa cells. High specificities of these antibodies were confirmed in this laboratory. The proteins associated with nuclear chromatin in interphase (Figure 7A). Upon entry into mitosis, however, RbAp46 and RbAp48 no longer associated with chromosomal DNA but re-associated before cell division: nuclear chromatin staining in telophase was particularly significant for RbAp46.

RNAi was performed for each protein individually and in combination to simultaneously target both homologs in order to determine whether, like their fission yeast counterpart, RbAp46 and RbAp48 are involved in recruiting CENP-A to centromeres. The levels of RbAp46 and RbAp48 in HeLa cells were greatly reduced 72 hr after adding specific siRNAs (Experimental Procedures) to the culture medium to induce RNAi knockdown (Figure 7B). No defect in CENP-A recruitment was apparent when RNAi was used to deplete RbAp46 or RbAp48 on their own (Figure 7C). When both molecules were targeted by simultaneous RNAi for both genes, the levels of the RbAp46 and RbAp48 proteins were not decreased by the same degree as that seen upon targeting of an individual molecule alone. However, despite this reduction in efficiency of depletion of RbAp46 and RbAp48, there was a dramatic and reproducible impact upon the ability of CENP-A to associate with kinetochores. The kinetochore signals of CENP-A were virtually abolished. Unfortunately the polyclonal antibodies against hMis6 did not work well enough in immunofluorescence microscopy to enable us to ask whether hMis6 also depended upon RbAp46/48 function for association with the kinetochores.

Note that the protein level of CENP-A was also reduced by RNAi treatment of HeLa cells that simultaneously depleted RbAp46 and RbAp48. RT-PCR for CENP-A in RbAp46/48 RNAi-treated cells showed that the decline in protein level did not arise from a decline in the abundance of CENP-A RNA transcript (Figure 7D). Monitoring the kinetics in the reduction of protein levels between 24 and 72 hr after RNAi ablation showed that CENP-A levels went into a slow decline after a rapid reduction of RbAp46/48 levels (Supplemental Figure S3 on *Cell* website). This suggests that the reduction in RbAp46/48 levels probably affected CENP-A stability because

(D) RT-PCR was done to estimate the levels of CENP-A transcripts in HeLa cells that had been subjected to single or double RNAi treatment. HeLa cells that had been treated with RNAi against CENP-A were used as control. No significant change was observed following single RNAi to ablate either RbAp46 or RbAp48 individually and double RbAp46 and RbAp48 in comparison with no RNAi.

(E) In HeLa cells simultaneously treated for RbAp46 and RbAp48 RNAi, micronuclei were not observed, whereas HeLa knockdown by CENP-A RNAi frequently showed micronuclei (indicated by arrows). Quantitative data are also shown.

(F) Interactions between kinetochore proteins (see text). Ams2 is a GATA-like factor that is required for the efficient loading of spCENP-A in fission yeast.

the protein that could not be incorporated into the centromeres was being degraded, rather than being a consequence of altered transcription of the gene.

The frequencies of mitotic and interphase cells were assessed by monitoring cell shape in cells in which 72 hr RNAi treatment had been followed by incubation for a further 18 hr in the presence or the absence of nocodazole (Noc). In contrast to those control cells without RNAi, the presence of Noc did not affect the frequency of mitotic cells if the cells had received a prior treatment with RNAi against RbAp46 and/or RbAp48 (data not shown). This indicated that many HeLa cells became defective in progression through interphase after RNAi of RbAp46 and/or RbAp48. After double RbAp46/48 knockdown, HeLa cells displayed very few of the micronuclei that become abundant after CENP-A RNAi treatment of HeLa cells (Figure 7E). The interphase phenotypes (infrequent occurrence of micronuclei) observed in HeLa cells after RNAi treatment that targeted both RbAp46 and RbAp48 were therefore rather distinct from that arising from CENP-A RNAi and probably occurred prior to the loss of CENP-A recruitment to kinetochores. These results strongly suggested that, like their fission yeast counterpart Mis16, RbAp46 and RbAp48 were upstream factors that were required for the recruitment of CENP-A to kinetochores.

Discussion

The present study was initiated by screening fission yeast for kinetochore mutants in an attempt to identify genes that are required for the recruitment of the two principal kinetochore proteins, Mis12/Mtw1 and spCENP-A. A systematic characterization of the dependency relationships between the ability of distinct kinetochore components to be recruited to centromeres indicated that Mis16 and Mis18 both acted as upstream factors for the kinetochore recruitment of CENP-A. By using RNAi in HeLa cells, we established that double knockdown of two human proteins that exhibit over 50% sequence identity to Mis16, RbAp46 and RbAp48, abolished kinetochore localization of CENP-A. Hence RbAp48-like WD40 proteins are essential factors that are required for the recruitment of CENP-A in both fission yeast and human cells. RbAp48/RbAp46/Mis16 are the first nuclear CENP-A recruitment factors to be identified that are conserved in human and fission yeast. Human Mis18 is also required for recruiting CENP-A, but a detailed analysis of Mis18 function will be reported elsewhere (Y. Fujita et al., submitted).

We provide evidence that Mis16 and Mis18, both essential for cell viability, function as upstream factors for the CENP-A kinetochore loading pathway. First, Mis16 and Mis18 are required for proper recruitment of a group of kinetochore proteins, CENP-A, Mis6/CENP-I, Mis15/Chl14, and Mis17 (but not for Mis12/Mtw1 and Mis14/Nsl1). The physical interaction of Mis16 with Mis18 is consistent with the mutual dependency between the function of each molecule for the recruitment of the other to kinetochores. The Mis16–Mis18 complex may be a part of the functional holo-complex. Secondly, and most importantly, with the exception of Mis16 and Mis18 themselves, these two molecules can be recruited to the kinetochore in the absence of any of these kinetochore protein functions. Third, a high copy number plasmid carrying CENP-A partly rescues the ts phenotype of the mutants implicated in the CENP-A loading pathway (but not mutants implicated in the Mis12 pathway). Fourth, the lack of a physical association between Mis16 and CENP-A is not inconsistent with an upstream role. Mis16 may indirectly affect CENP-A as a downstream target. However, the level of immunoprecipitable Cnp1-HA in the 0.2 M NaCl supernatants used for immunoprecipitation was not great and so it may have been difficult to detect a direct interaction under the condition used here. Similarly, Mis16 or Mis18 might directly interact with Cnp1 bound to chromatin, but such an interaction would not be detected in our assays. Alternatively, other kinetochore proteins such as Mis6, Mis15, or Mis17 or unidentified proteins may directly interact with CENP-A.

What then is known about RbAp48/RbAp46- and Mis16-related proteins? They belong to a particular class of WD40 proteins (WD stands for Trp and Asp, and 40 for the unit of repeat amino acids), many of which act in different ways on chromatin. RbAp46/48 is rather abundant and was found to be a ubiquitous binding partner of retinoblastoma (RB) tumor suppresser protein (Qian et al., 1993) and a component of the human chromatin-assembly factor-1 (CAF-1) complex that promotes the assembly of nucleosomes onto newly replicated DNA (Verreault et al., 1996; Krude, 1999). The fly RbAp46/48-like protein is a component of chromatin-remodeling complex NURF (Martinez-Balbas et al., 1998). In plants *Arabidopsis*, AtMSI1 that is similar to RbAp46/48 is implicated in gene silencing, a part of an epigenetic process (Hennig et al., 2003). As gene silencing is believed to be caused by the immobilization of nucleosomes that would inhibit the access for active gene expression and require histone modifications, such as deacetylation or methylation, it is gratifying that RbAp46/48-like proteins are reported to be a component of histone deacetylation complex (Nakayama et al., 2003; Furuyama et al., 2003). One model that has been proposed (Henikoff, 2003) is that RbAp46/48-like proteins perform their tasks during replication-coupled nucleosome assembly and hold out exposed histones (the tetramer of histones H3 and H4) for modification and chromatin remodeling. However, a plasmid carrying the gene for Prw1, a fission yeast WD40 in the histone deacetylation complex that is similar to Mis16, failed to suppress the *mis16* mutant phenotype, so it would appear that Mis16 may not be directly involved in Clr6-dependent histone deacetylation. In addition, Clr6 showed no influence over the acetylation pattern of histones in the central cores of centromeres (see below).

The question of how kinetochore chromatin assembly is affected by Mis16 (and Mis18) was addressed by CHIP experiments using antibodies against acetylated histones H3 and H4. In wild-type cells, any of four antibodies were barely capable of precipitating the central centromere cnt and imr regions but efficiently precipitated the outer centromere dg probe and the lys1 gene sequence. In both *mis16* and *mis18* mutants, however, there was a striking increase in the abundance of acetylated histones within the central centromere regions. Such drastic changes were specific to the central centromere. In *mis12* and *clr6* mutants, such changes were

not observed. We concluded that the central centromere is highly deacetylated in wild-type, and that the maintenance of such a state required Mis16 and Mis18 function. It remains to be determined whether the Mis16 and Mis18 complex directly affected the state of histone acetylation as a part of a deacetylase. *S. pombe* has six histone deacetylases that include the one that contains Clr6, and it will be of considerable interest to identify which deacetylase is functionally related to Mis16 and Mis18.

Mis16 is present throughout the nuclear chromatin and may not act solely at kinetochores. It may interact with multiple proteins in addition to Mis18. The binding of Mis18 to Mis16 may confer the specificity for acting at centromeres. This model may explain our results in fission yeast and fit with the situation in HeLa cells. Single RbAp48 and RbAp46 RNAi did not reduce CENP-A kinetochore signals, but after single RNAi treatment of either homolog, HeLa cells ceased to grow, suggesting that RbAp46 and RbAp48 have essential functions that are distinct from CENP-A recruitment. However, only the double RNAi greatly diminished the loading of CENP-A onto kinetochores, indicating that human Mis18 may functionally interact with both RbAp48 and RbAp46. Mis16/RbAp46/48 may have multiple tasks in chromatin assembly and remodeling, one of them being to facilitate the recruitment of CENP-A or CENP-A-containing histone oligomers to the site of kinetochore chromatin by interacting with Mis18.

The seven kinetochore-defective mutants isolated through cytological screening of over 1000 ts strains in this study defined five new genetic loci, *mis14–mis18*. All of these mutants were defective in the specialized chromatin structure of the central centromere region and displayed unequal segregation in anaphase. Figure 7F shows a summary of the genetic interactions revealed as high-copy suppression (black arrows) and physical interactions (blue lines) alongside the localization dependency relationships (green arrows). Mis14 belongs to the Mis12 group, while Mis15, Mis16, Mis17, and Mis18 form the CENP-A group that also includes Mis6 and Ams2. Ams2, a GATA-like element, genetically interacts with Mis12 and Mis14 and links the two groups. We showed that Mis12 and Mis14 formed a complex, while Mis6, Mis15, and Mis17 constituted another complex. These results are consistent with the recent reports of the kinetochore protein complexes of *S. cerevisiae* (Pinsky et al. 2003; Scharfenberger et al., 2003; Nekrasov et al., 2003; Westermann et al., 2003; De Wulf et al., 2003; Cheeseman et al., 2002). In these studies, the Mtw1 (Mis12-like) complex was shown to contain Nsl1 (Mis14) and two other proteins. The Ctf19 complex contained Ctf3 (Mis6) and Chl4 (Mis15). Although no extensive sequence similarity existed between Ctf19 and Mis17, Mis17 is possibly a functional counterpart of Ctf19 in the complex. Fission yeast kinetochore formation thus requires at least three complexes (circles in Figure 7F), two of which are also found in budding yeast.

Experimental Procedures

Strains, Media, and Culture of Nitrogen-Starved Cells

S. pombe strains were derived from haploid wild-type *972* (h^-) and *975*(h^+). The complete YPD, the minimal EMM2, and the sporulation medium SPA are described previously (Moreno et al., 1991). Transformation was done using the lithium method (Ito et al., 1983). Cell number was measured by the Sysmex F-800 (Toa Med Elec Co). For nitrogen starvation, cells grown in EMM2 were suspended in EMM2-NH_4Cl at 26°C for 24 hr. For the release from the G1 arrest, cells were diluted to an appropriate concentration in YPD. HeLa cells were grown at 37°C in D-MEM (GIBCO) supplemented with 10% FBS, 1% penicillin-streptomycin, and 1% antibiotic-antimycotic.

Plasmids and Gene Handling

Multicopy vector pSK248 containing the budding yeast *LEU2* was used to clone the *S. pombe* genes that could complement the ts phenotype of mutants. For integration of the genomic DNA onto chromosome, pYC6 and pYC11 that contained the *S. pombe ura4*$^+$ gene and the budding yeast *LEU2*, respectively, but lacked a replication origin were used (Chikashige et al., 1989).

Isolation of ts Mutants

The procedures described by Takahashi et al. (1994) were followed. *S. pombe* strain h^- *leu1 GFP-eat1*$^+$ containing the integrated GFP-*eat1*$^+$ gene whose product is located in the nuclear chromatin was used for mutagenesis by N-methyl-N′-nitrosoguanidine (NTG). The *S. pombe* culture treated with NTG was grown and plated, followed by replica plating. Strains that could grow at 26°C but not at 36°C were selected and streaked. These ts candidate strains were stored in glycerol. One thousand fifteen ts strains were obtained from 200,000 colonies. Seven mutants (53, 68, 262, 271, 362, 634, 818) displayed a chromosome missegregation phenotype that resulted in large and small daughter nuclei at 36°C. The temperature sensitivity of all the seven strains showed 2:2 segregation pattern in tetrad analysis, indicating that a single mutation is responsible for the mutant phenotype.

Gene Cloning and myc- or GFP-Tagged Genes

The genomic DNA library was transformed into *mis14–mis18* mutants in order to identify the mutant genes. Transformants were collected and plasmids were recovered. As the whole genome sequence of *S. pombe* has been determined, the sequences at the end of the inserts in these clones were used to define the genomic sequences cloned in the complementing DNA fragments. Introns were confirmed by PCR amplification of cDNA. Plasmids were recovered from transformants of *mis14–271*. Subcloning established that Spac688.02c (25 kb from *scn1* locus) was responsible for complementation. Tetrad dissection indicated that *scn1* and *mis14–271* were only 4.2 cM apart, supporting the conclusion that the *mis14*$^+$ gene was identical to Spac688.02c. Transformation and subcloning followed by tetrad dissection showed that pi022 was the gene encoding Mis15. Although the database indicated that pi022 had two introns, cDNA sequencing showed that the second one was not correctly assigned. The corrected *mis15*$^+$ sequence codes for a 409 amino acid polypeptide (calculated MW, 47.4 kDa, pI 6.54). Cloning and tetrad dissection established that a single genetic locus Spcc1672.10 encoded Mis16. The *mis16* locus is linked to *cut15–85* (24.2 cM). Gene cloning and tetrad dissection established that the *mis17*$^+$ gene was identical to Spbc21.01. Mis17 encodes a 441 amino acid protein (calculated MW, 49.6 kDa; pI, 4.86). The *mis18*$^+$ gene was identified as Spcc970.12. The *mis18–262* and *mis18–818* mutant genes contained G117D and T49A substitutions, respectively. To tag the C terminus by myc or GFP, the termination codons of *mis14*$^+$*–mis18*$^+$ genes were changed to the NotI site so as to incorporate 8Myc or GFP and the polyA terminal sequences of the *nmt1*$^+$ gene (Maundrell, 1990). The S65T mutant form of GFP was used (Heim et al., 1995). Southern hybridization confirmed the correct integration of the tagged sequence. The Myc-tagged Mis14, Mis15, and Mis16 produced the bands with expected molecular weights (46 kDa, Mis14-myc; 62 kDa, Mis15-myc; 80 kDa, Mis16-myc).

Microscopy and FACScan

DAPI staining was done as described (Adachi and Yanagida, 1989). To observe cells that expressed the tagged GFP protein, cells were adhered to glass funnel filter and fixed by immersion in 100% methanol at −80°C. After 30 min, PBS (phosphate buffer saline) was added

to cells for washing cells until 30% methanol dilution. To observe the pericentromeric DNA, LacI-GFP-NLS was expressed in the presence of thiamine (Goshima et al., 1999) and bound to the LacI binding sequences at the *lys1* locus near CEN1 (Nabeshima et al., 1997; Straight et al., 1996). The procedures for immunofluorescence microscopy of HeLa cells were described (Goshima et al., 2003). Anti-RbAp48 and anti-RbAp46 polyclonal antibodies were from Calbiochem. For estimation of the DNA content, the Becton Dickinson FACScan apparatus was used.

MNase Digestion, CHIP, and Immunoprecipitation

The MNase digestion was done using three probes described previously (Takahashi et al., 1992). The CHIP method was also performed as described (Saitoh et al., 1997). For immunoprecipitation, cell extracts were prepared with the extraction buffer (25 mM HEPES-KOH at pH7.5, containing 200 mM NaCl, 10% glycerol, 0.2% NP-40 and protease inhibitors, 1 mM PMSF, and 1% Trasylol). Immunoprecipitation was done using anti-Myc antibody (9E10, Calbiochem), anti-HA antibody (12CA5, Roche), and anti-GFP antibody (Roche) conjugated with protein A-Sepharose. Antibodies against acetylated histones H3 and H4 were purchased from Upstate Inc.

RNAi Method

The siRNA (Elbashir et al., 2001) was synthesized for RNAi of RbAp48 (5′-GCCACUCAGUUGAUGCUCATT-3′) and RbAp46 (5′-GGAGAA GUAAACCGUGCUCTT-3′) by JbioS. The procedures of cell culture and transfection were based on Elbashir et al. (2001) and Harborth et al. (2001) using Oligofectamine (Invitrogen). Cells for immunoblotting and fluorescence microscopy were collected 72 hr after transfection.

Acknowledgments

We are greatly indebted to Chikashi Shimoda and Kinya Yoda for genomic library and kinetochore protein antibodies. We are most grateful to Kevin Sullivan, Iain Hagan, and Andrew Murray for critically reading the manuscript. This work was supported by the COE Scientific Research Grant, and T. H., O. I., and Y. A. were supported by the 21st Century COE grant of the Graduate School of Biostudies, from the Ministry of Education, Culture, Sports, Science and Technology of Japan.

Received: January 23, 2004
Revised: August 26, 2004
Accepted: August 30, 2004
Published: September 16, 2004

References

Adachi, Y., and Yanagida, M. (1989). Higher order chromosome structure is affected by cold-sensitive mutations in an *S. pombe* gene *crm1*$^{+}$ which encodes a 115-kd protein preferentially localized in the nucleus and at its periphery. J. Cell Biol. *108*, 1195–1207.

Cheeseman, I.M., Anderson, S., Jwa, M., Green, E.M., Kang, J., Yates, J.R., 3rd, Chan, C.S., Drubin, D.G., and Barnes, G. (2002). Phospho-regulation of kinetochore-microtubule attachments by the Aurora kinase Ipl1p. Cell *111*, 163–172.

Chen, E.S., Saitoh, S., Yanagida, M., and Takahashi, K. (2003). A cell cycle-regulated GATA factor promotes centromeric localization of CENP-A in fission yeast. Mol. Cell *11*, 175–187.

Chikashige, Y., Kinoshita, N., Nakaseko, Y., Matsumoto, T., Murakami, S., Niwa, O., and Yanagida, M. (1989). Composite motifs and repeat symmetry in S. pombe centromeres: direct analysis by integration of NotI restriction sites. Cell *57*, 739–751.

De Wulf, P., McAinsh, A.D., and Sorger, P.K. (2003). Hierarchical assembly of the budding yeast kinetochore from multiple subcomplexes. Genes Dev. *17*, 2902–2921.

Earnshaw, W.C., and Migeon, B.R. (1985). Three related centromere proteins are absent from the inactive centromere of a stable isodicentric chromosome. Chromosoma *92*, 290–296.

Elbashir, S.M., Harborth, J., Lendeckel, W., Yalcin, A., Weber, K., and Tuschl, T. (2001). Duplexes of 21-nucleotide RNAs mediate RNA interference in cultured mammalian cells. Nature *411*, 494–498.

Euskirchen, G.M. (2002). Nnf1p, Dsn1p, Mtw1p, and Nsl1p: a new group of proteins important for chromosome segregation in Saccharomyces cerevisiae. Eukaryot. Cell *1*, 229–240.

Furuyama, T., Tie, F., and Harte, P.J. (2003). Polycomb group proteins ESC and E(Z) are present in multiple distinct complexes that undergo dynamic changes during development. Genesis *35*, 114–124.

Goshima, G., Kiyomitsu, T., Yoda, K., and Yanagida, M. (2003). Human centromere chromatin protein hMis12, essential for equal segregation, is independent of CENP-A loading pathway. J. Cell Biol. *160*, 25–39.

Goshima, G., and Yanagida, M. (2000). Establishing biorientation occurs with precocious separation of the sister kinetochores, but not the arms, in the early spindle of budding yeast. Cell *100*, 619–633.

Goshima, G., Saitoh, S., and Yanagida, M. (1999). Proper metaphase spindle length is determined by centromere proteins Mis12 and Mis6 required for faithful chromosome segregation. Genes Dev. *13*, 1664–1677.

Harborth, J., Elbashir, S.M., Bechert, K., Tuschl, T., and Weber, K. (2001). Identification of essential genes in cultured mammalian cells using small interfering RNAs. J. Cell Sci. *114*, 4557–4565.

Heim, R., Cubitt, A.B., and Tsien, R.Y. (1995). Improved green fluorescence. Nature *373*, 663–664.

Henikoff, S. (2003). Versatile assembler. Nature *423*, 814–815, 817.

Henikoff, S., Ahmad, K., Platero, J.S., and van Steensel, B. (2000). Heterochromatic deposition of centromeric histone H3-like proteins. Proc. Natl. Acad. Sci. USA *97*, 716–721.

Hennig, L., Taranto, P., Walser, M., Schonrock, N., and Gruissem, W. (2003). Arabidopsis MSI1 is required for epigenetic maintenance of reproductive development. Development *130*, 2555–2565.

Ito, H., Fukuda, Y., Murata, K., and Kimura, A. (1983). Transformation of intact yeast cells treated with alkali cations. J. Bacteriol. *153*, 163–168.

Jin, Q.W., Pidoux, A.L., Decker, C., Allshire, R.C., and Fleig, U. (2002). The mal2p protein is an essential component of the fission yeast centromere. Mol. Cell. Biol. *22*, 7168–7183.

Krude, T. (1999). Chromatin assembly during DNA replication in somatic cells. Eur. J. Biochem. *263*, 1–5.

Martinez-Balbas, M.A., Tsukiyama, T., Gdula, D., and Wu, C. (1998). Drosophila NURF-55, a WD repeat protein involved in histone metabolism. Proc. Natl. Acad. Sci. USA *95*, 132–137.

Maundrell, K. (1990). nmt1 of fission yeast. J. Biol. Chem. *265*, 10857–10864.

Measday, V., Hailey, D.W., Pot, I., Givan, S.A., Hyland, K.M., Cagney, G., Fields, S., Davis, T.N., and Hieter, P. (2002). Ctf3p, the Mis6 budding yeast homolog, interacts with Mcm22p and Mcm16p at the yeast outer kinetochore. Genes Dev. *16*, 101–113.

Moreno, S., Klar, A., and Nurse, P. (1991). Molecular genetic analysis of fission yeast Schizosaccharomyces pombe. Methods Enzymol. *194*, 795–823.

Nabeshima, K., Saitoh, S., and Yanagida, M. (1997). Use of green fluorescent protein for intracellular localization in living fission yeast cells. Methods Enzymol. *283*, 459–471.

Nakayama, J., Xiao, G., Noma, K., Malikzay, A., Bjerling, P., Ekwall, K., Kobayashi, R., and Grewal, S.I. (2003). Alp13, an MRG family protein, is a component of fission yeast Clr6 histone deacetylase required for genomic integrity. EMBO J. *22*, 2776–2787.

Nekrasov, V.S., Smith, M.A., Peak-Chew, S., and Kilmartin, J.V. (2003). Interactions between centromere complexes in Saccharomyces cerevisiae. Mol. Biol. Cell *14*, 4931–4946.

Palmer, D.K., O'Day, K., Wener, M.H., Andrews, B.S., and Margolis, R.L. (1987). A 17-kD centromere protein (CENP-A) copurifies with nucleosome core particles and with histones. J. Cell Biol. *104*, 805–815.

Pidoux, A.L., Richardson, W., and Allshire, R.C. (2003). Sim4: a novel

fission yeast kinetochore protein required for centromeric silencing and chromosome segregation. J. Cell Biol. *161*, 295–307.

Pinsky, B.A., Tatsutani, S.Y., Collins, K.A., and Biggins, S. (2003). An Mtw1 complex promotes kinetochore biorientation that is monitored by the Ipl1/Aurora protein kinase. Dev. Cell *5*, 735–745.

Pot, I., Measday, V., Snydsman, B., Cagney, G., Fields, S., Davis, T.N., Muller, E.G., and Hieter, P. (2003). Chl4p and iml3p are two new members of the budding yeast outer kinetochore. Mol. Biol. Cell *14*, 460–476.

Qian, Y.W., and Lee, E.Y. (1995). Dual retinoblastoma-binding proteins with properties related to a negative regulator of ras in yeast. J. Biol. Chem. *270*, 25507–25513.

Qian, Y.W., Wang, Y.C., Hollingsworth, R.E., Jr., Jones, D., Ling, N., and Lee, E.Y. (1993). A retinoblastoma-binding protein related to a negative regulator of Ras in yeast. Nature *364*, 648–652.

Saitoh, S., Takahashi, K., and Yanagida, M. (1997). Mis6, a fission yeast inner centromere protein, acts during G1/S and forms specialized chromatin required for equal segregation. Cell *90*, 131–143.

Scharfenberger, M., Ortiz, J., Grau, N., Janke, C., Schiebel, E., and Lechner, J. (2003). Nsl1p is essential for the establishment of bipolarity and the localization of the Dam-Duo complex. EMBO J. *22*, 6584–6597.

Stoler, S., Keith, K.C., Curnick, K.E., and Fitzgerald-Hayes, M. (1995). A mutation in CSE4, an essential gene encoding a novel chromatin-associated protein in yeast, causes chromosome nondisjunction and cell cycle arrest at mitosis. Genes Dev. *9*, 573–586.

Straight, A.F., Belmont, A.S., Robinett, C.C., and Murray, A.W. (1996). GFP tagging of budding yeast chromosomes reveals that protein-protein interactions can mediate sister chromatid cohesion. Curr. Biol. *6*, 1599–1608.

Takahashi, K., Murakami, S., Chikashige, Y., Funabiki, H., Niwa, O., and Yanagida, M. (1992). A low copy number central sequence with strict symmetry and unusual chromatin structure in fission yeast centromere. Mol. Biol. Cell *3*, 819–835.

Takahashi, K., Yamada, H., and Yanagida, M. (1994). Fission yeast minichromosome loss mutants mis cause lethal aneuploidy and replication abnormality. Mol. Biol. Cell *5*, 1145–1158.

Takahashi, K., Chen, E.S., and Yanagida, M. (2000). Requirement of Mis6 centromere connector for localizing a CENP-A-like protein in fission yeast. Science *288*, 2215–2219.

Verreault, A., Kaufman, P.D., Kobayashi, R., and Stillman, B. (1996). Nucleosome assembly by a complex of CAF-1 and acetylated histones H3/H4. Cell *87*, 95–104.

Westermann, S., Cheeseman, I.M., Anderson, S., Yates, J.R., 3rd, Drubin, D.G., and Barnes, G. (2003). Architecture of the budding yeast kinetochore reveals a conserved molecular core. J. Cell Biol. *163*, 215–222.